

Evidence of Conformational Heterogeneity for Carbohydrate Mimetics. NMR Study of Methyl β -C-Lactoside in Aqueous Solution

Gilles Rubinstenn,^{†,‡} Pierre Sinaÿ,[‡] and Patrick Berthault^{*,†}

Laboratoire Commun de RMN, DRECAM/SCM, CEA Saclay, F-91191 Gif sur Yvette cedex, France, and
Département de Chimie, Ecole Normale Supérieure, 24 rue Lhomond, F-75231 Paris cedex 05, France

Received: September 11, 1996; In Final Form: January 31, 1997[⊗]

The structure and internal dynamics of methyl β -C-lactoside in aqueous solution has been derived by ¹H NMR and molecular modeling. A simulated annealing procedure under nuclear Overhauser effect (nOe) restraints produced a family of 50 structures. However, no single one of them was satisfactory; for each a rather important deviation between experimental and simulated data was found. Examination of the H–H correlation times given by off-resonance ROESY and comparison of the experimental and simulated coupling constants related to the interglycosidic dihedral angles indicated that the problem arose from internal mobility around the ψ angle. Using the result of a ϕ/ψ map, we have tried to find the best agreement between experimental and back-calculated nOe distances with two families having the same angle ϕ but different ψ values. The best fit is obtained for 40% of ($\phi_A = 295^\circ$; $\psi_A = 300^\circ$) and 60% of ($\phi_B = 295^\circ$; $\psi_B = 130^\circ$). This result represents the first step toward comparison of the structure and dynamics of C- and O-glycosides in aqueous solution.

Introduction

Recently, the advent of a new class of carbohydrate mimetics, the C-saccharides,¹ has opened a wide research area for the study of the relationships between their structural and dynamic properties and their biological activity. Compared to their O-glycosidic natural counterparts, the C-disaccharides, for which the interglycosidic bond has been replaced by a methylene bridge (Figure 1), exhibit a higher chemical and biochemical stability. However, up to now it is not clear whether or not such a modification leads to important repercussions of the properties of these synthetic derivatives. First, the electroacceptor oxygen atom is substituted by a noncharged carbon atom (the anomeric center is subjected to a formal reduction). Second, the steric hindering of the interglycosidic bond is modified, as well as the involved bond lengths and bond angles.

In the hypothesis that the C-disaccharides are structural mimetics of their natural analogues, it would become possible to derive the biological properties of the latter compounds from a study of the former ones. Y. Kishi et al. have shown in many examples this similitude for what concerns the anomeric effect² and the exoanomeric effect³. Hartree–Fock calculations were also in agreement with this.⁴ Moreover, all these results have been confirmed by molecular recognition assays in the case of analogues of blood group determinants.⁵

For such a study, it is necessary not only to have access to efficient techniques for the synthesis of these compounds but also to find adequate biological tests, as well as dedicated methods for determination of their structure and their internal dynamics. Owing to its ability to give detailed information about the structural and dynamic properties of molecules in solution, liquid-state high-resolution NMR is a powerful tool for understanding the major biological role of carbohydrates.⁶ For the O-glycosidic series, the presence of the interglycosidic

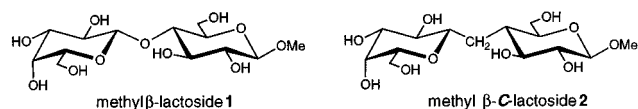


Figure 1. Molecular drawings of methyl β -lactoside **1** and its C-analogue methyl β -C-lactoside **2**.

bond, however, hampers the ¹H NMR study. First, it renders impossible the scalar *through-bond* magnetization transfer from one unit to the other. Second, it considerably reduces the number of dipolar *through-space* data between the two units. The two techniques that give information on the geometry and the dynamics around the interglycosidic bond, namely, measurement of the long-range ¹³C–H couplings⁷ and of the ¹³C longitudinal relaxation times,⁸ are rather insensitive and known to give inaccurate results. From this point of view, the C-disaccharides present an important advantage over the O-disaccharides, since they have two hydrogen atoms in a very strategic position. This enables the recording of data about the ϕ, ψ interglycosidic dihedral angles⁹ (H–H scalar coupling constants related to them through Karplus-type relationships), as well as additional interproton distance constraints.

It is known that for medium-sized molecules in aqueous solution at ambient temperature, the ¹H longitudinal cross-relaxation rate is small, whatever the interproton distance, which does not allow an easy determination of geometric constraints through this method. Furthermore, the classical ROESY experiment¹⁰—initially designed to overcome this problem—suffers from superposition of dipolar *through-space* effects and unwanted Hartmann–Hahn *through-bond* coherence transfers.¹¹ This phenomenon is frequent for sugars, where strong coupling conditions can be encountered, since the resonances are in a rather narrow spectral range.

We have recently suggested a new approach using strong off-resonance rf irradiation as a spin-lock in the mixing time of a ROESY pulse scheme¹² and have shown that the usual drawbacks rendering the experiment not easily quantitative (offset dependence and Hartmann–Hahn transfers) were suppressed. Moreover, playing with the rf offset and/or the rf field

* To whom correspondence should be addressed (e-mail address: Patrick.Berthault@Cea.fr).

[†] CEA Saclay.

[‡] Ecole Normale Supérieure.

[⊗] Abstract published in *Advance ACS Abstracts*, March 1, 1997.

strength, we have developed a method for obtaining simultaneously structural and motional data per pair of protons without the usual approximate assumptions.¹³ This has been applied to the study of a mixed C/O-trisaccharide analogue of Lewis^X in aqueous solution.¹⁴ However, although very promising results have been found for the capability of the method to accurately determine its 3D solution structure, one of the conclusions was that it existed in solution in the form of a unique family, with substantial conformational rigidity. It seemed, therefore, interesting to apply our method to the study of a more flexible molecule. We have developed a new synthetic pathway, using radical cyclization, for a more efficient production of methyl- β -C-lactoside¹⁵ (compound **2** in Figure 1), and this compound is ideal for the assessment of the quality of the approach.

Material and Methods

NMR. Acquisition. Compound **2** was dissolved in D₂O, freeze-dried, and redissolved in this solvent. The final concentration was 15 mM. The NMR study was performed at 22 °C on two spectrometers: a Bruker DRX500 delivering a field of 11.7 T and a Bruker DRX600 (field of 14 T). The ¹H spectral assignment was confirmed by double quantum-filtered COSY¹⁶ and multistep relayed COSY¹⁷ experiments.

Two-dimensional off-resonance ROESY experiments with a trapezoidal shape for the spin-lock pulse¹⁸ and reduction of the angular dispersion through irradiation at opposite offsets¹⁹ allowed the recording of quantitative cross-relaxation peaks. The rf field strength was ca. 10 kHz. A quantity of 192 free induction decays (FIDs) of 2048 points constituted the acquisition matrix. Each *t*₁ increment consisted of 32 scans with 3.2 s for the recovery delay between them. The total time of each experiment was ca. 2 h 30 min. A total of 36 experiments were performed, corresponding to 9 angles between the static field and the effective field axes ($\theta = 10^\circ, 20^\circ, 25^\circ, 30^\circ, 35^\circ, 40^\circ, 45^\circ, 47^\circ, \text{ and } 54.7^\circ$) and 4 mixing times (30, 50, 75, and 100 ms). For a further gain in precision, some 1D off-resonance ROESY data were also recorded with selective excitation of a single signal by a shaped 270° Gaussian pulse.²⁰ Three protons were thereby irradiated: H_{link}, H'_{link}, (the two protons of the methylene linker), and H1'. A quantity of 11 angles θ (5°, 10°, 15°, 20°, 25°, 30°, 35°, 40°, 45°, 50°, and 54.7°) and 5 mixing times (30, 50, 75, 100, and 150 ms) were retained for each of them.

Processing. After apodization of the FIDs with a cosine function in both dimensions, double Fourier transformation, and zero-filling to 512 points in the indirect dimension, the phase of the resulting maps was manually corrected and then an automatic base line correction applied. Details of the procedure transforming the cross-peak volumes into distance constraints have already been described in refs 12–14 and are only summarized in the Appendix. The normalized peak volumes have been measured and plotted as a function of the mixing time. The effective cross-relaxation rates have been extracted for each angle θ by the initial slope approximation. They have then been plotted as a function of θ and fitted with the theoretically expected curve to get the accurate values of the pure longitudinal and transverse relaxation rates through the Marquard algorithm.²¹ For each proton pair, these two values have been transformed into a geometrical parameter (the interproton distance *r*_{ij}) and a dynamic parameter (the correlation time of the H–H vector τ_{cij}).¹³

Molecular Modeling. The experimental interproton distances have been introduced in a simulated annealing procedure in XPLOR 3.1.²² To take into account the experimental error, the lower and upper bounds have been set to ± 0.2 Å. Starting from a template structure exhibiting nonaberrant covalent terms,

a high-temperature dynamics of 1000 K during 10 ps is simulated with progressive introduction of the nOe restraints and decrease of the weight of the van der Waals term. An 8 ps slow cooling step follows during which all energetic terms are set to their usual values. This procedure is repeated 50 times with random initial atomic velocities at the beginning of the high-temperature dynamics. The nOe distances have been back-calculated after averaging in r^{-6} over all 50 resulting structures.

The experimental values of the H1'–H_{link} and H1'–H'_{link} coupling constants and the respective chemical shifts of the interglycosidic protons enable the identification of H_{link} as pro-S. The results of the simulated annealing procedure, which has been performed without any stereospecific assignment, confirm this prochiral configuration.

An energy map ϕ/ψ has been calculated with the DISCOVER program²³ using the CFF91 force field²⁴ with preliminary automatic assignment of the atom types and charges. For the map, each of these dihedral angles has been varied by steps of 3° and kept fixed each time by introduction of fictive forces. A 1000-steps truncated Newton–Raphson minimization has been applied for each point of the map. The coupling constants involving the interglycosidic link have then been back-calculated according to the Karplus relationship parametrized by Haasnoot et al.²⁵

Results and Discussion

For each proton pair, the measurement of the effective cross-relaxation rate as a function of the angle θ between the axis of the field effectively experienced by the nuclei and the static field axis enables the recording of a structural parameter (the interproton distance *r*_{ij}) and a dynamic parameter (τ_{cij} , “correlation time of the pair” indicative of the reorientational motion of the proton pair). The important points are (1) that no internal distance reference is needed, in contrast to the classical method, (2) the model that we use is that the motion of each proton pair can be adequately described by an independent Lorentzian autocorrelation function (no hypothesis is made on the global motion of the molecule), (3) distances and correlation times are obtained in the same experiment, and therefore, less bias due to the dependence of one on the other is introduced. The complementary use of 2D and 1D off-resonance ROESY has thereby enabled the accurate determination of 19 local correlation times and 19 H–H distances used as constraints in molecular modeling. Of them, two are purely interglycosidic and nine involve a proton of the methylene bridge and a proton of a pyranosidic ring. Owing to spectral overlap of the H5 and H6 signals, some of these distances are only average distances between groups of atoms.

The introduction of these distance constraints in the simulated annealing procedure leads to 50 structures showing a relatively high degree of similarity among them: the rmsd of their atomic coordinates is 0.3 Å when the carbon and intraring oxygen atoms are considered. When the interproton distances are back-calculated and r^{-6} averaged over all 50 structures, the rmsd between the experimental and simulated data is 0.18 Å. Figure 2A represents the correspondence between the experimental data and the simulated ones. This rmsd is higher than the corresponding value found for the study of a trisaccharide analogue of Lewis^X (0.15 Å, Figure 2C and ref 14), although the average number of constraints per proton is lower. Moreover, all structures exhibit at least one nOe violation greater than 0.2 Å. Also, a comparison of the theoretical vicinal coupling constants around the interglycosidic link estimated from the ϕ and ψ dihedral angles through a simple Karplus-type relationship with the experimental data is informative (Table 1, columns 1 and

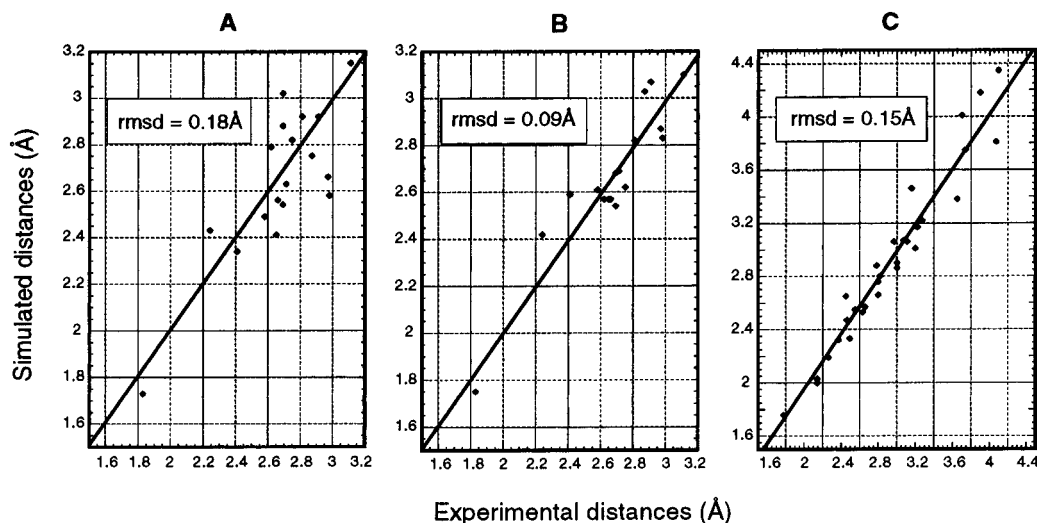


Figure 2. Maps representing the agreement between simulated distances and experimental distances: (A) results for the simulated annealing procedure (after averaging r^{-6} over the 50 obtained structures) in the case of the *C*-lactoside; (B) results for two structural families in the case of the *C*-lactoside; (C) results for the simulated annealing procedure in the case of the *C*-fucosyllactoside (according to ref 14, after averaging r^{-6} over the 50 obtained structures).

TABLE 1: Experimental and Simulated Interglycosidic Coupling Constants

coupling constants	exptl data	one-population model ^a	best two-population model ^b
$J_{H1'/H_{link}}$	2.2	1.0	2.0
$J_{H1'/H'_{link}}$	9.7	10.5	10.8
$J_{H4/H_{link}}$	4.9	9.6	4.8
$J_{H4/H'_{link}}$	3.5	6.6	3.2

^a $\Phi = 287^\circ$, $\Psi = 24^\circ$. ^b 40% ($\Phi_A = 295^\circ$, $\Psi_A = 300^\circ$) + 60% ($\Phi_B = 295^\circ$, $\Psi_B = 130^\circ$).

2). Whereas the experimental and calculated coupling constants characterizing the dihedral angle ϕ are in accord (rows 1 and 2), the situation is different for ψ (rows 3 and 4). In the case of ϕ , the coupling constants represent extrema of the semiempirical law, which should imply a relative rigidity around this dihedral angle. Conversely, the values observed in the spectrum for the coupling constants corresponding to ψ could reveal the presence of several conformations in solution. We have also observed that the six H–H distances that strongly depend on ψ , i.e., $H_{link}-H4$, $H'_{link}-H4$, $H_{link}-H3$, $H'_{link}-H3$, $H1'-H4$, and $H1'-H3$, show the biggest discrepancies between experimental and simulated data (rmsd = 0.23 Å).²⁶ This is compared with a recent report on a mixture of free α/β -*C*-lactose published by J. Jiménez-Barbero and co-workers²⁷ that seemed to indicate that several conformational families were involved in the apparent dynamics of the compounds. For these authors, the ϕ, ψ parameters were found to be identical with those of the natural lactose, but the ratio of these families was significantly different.²⁸ However, their results obtained by molecular modeling (MM3²⁹) showed poor compatibility with the experimental data determined by steady-state nOe experiments.³⁰

To confirm or disprove the hypothesis of an internal motion around ψ , we have examined the dynamic parameter obtained by the NMR protocol used, i.e., the local correlation time per proton pair. We have separated them in two classes: the data corresponding to the mobility around ψ (class I) and the others (class II). The histogram in Figure 3 clearly shows that the correlation times in class I are inferior to those of class II, which may indicate the presence of internal dynamics involving rotation around ψ . The mean value for the correlation times of class I is 0.15 ns, that of class II is 0.18 ns. The difference

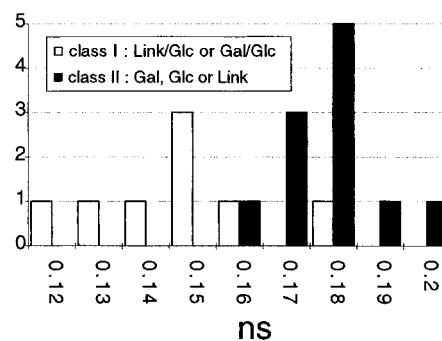


Figure 3. Histogram of the correlation times of proton pairs separated in two groups: those related to the mobility around ψ (set I) and the others (set II).

between these values is greater than the rmsd of the total set (0.02 ns). Applying the student's *t*-test, which measures the probability that two small discrete ensembles come from two subjacent populations having the same average,²¹ gives a result of 0.15%. This illustrates the significantly distinct character of the classes and therefore shows that they are related to motions on a different time scale. Note that the severe spectral overcrowding does not allow us to ensure for all protons that the ratio σ/ρ (sum of the cross-relaxation rates over direct relaxation rate) equals 0.5 for $\theta = 54.7^\circ$, which would indicate that no mechanism other than the dipolar one influences relaxation. The second important remark is that for these correlation time values at 11.7 T $\omega\tau_c$ is around 0.5. It falls in a region where the ratio σ/μ is subjected to important variations as a function of τ_c . So we can expect that our sensor for internal motion is sensitive and precise in this case.

The ϕ/ψ map built with the CFF91 force field²⁴ is displayed in Figure 4. It confirms the presence of several energy minima. Their positions are in accord with the results found by Jiménez-Barbero et al.,²⁷ but their depths are very different, which illustrates the difficulty of accurately evaluating the energy of a small molecule. It is also noteworthy that the most important minima appear in a region compatible with the value of ϕ found by simulated annealing. Given the shape of the energy landscape, we have tried to determine whether the use of two populations having different ψ values could improve the fit with

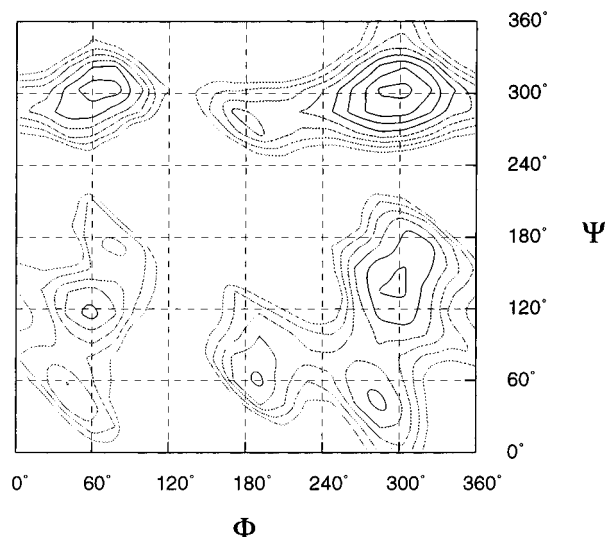


Figure 4. Isoenthalpic map for methyl β -C-lactoside obtained by variation of the Φ and Ψ angle values (3° steps) and minimization at each point with 1000 steps of truncated Newton–Raphson. Contours are given for every 1 kcal mol $^{-1}$.

the experimental data. In particular, we have done the following calculation. By keeping the more localized minimum ($\phi = 295^\circ$; $\psi = 300^\circ$: population A), we have calculated the rmsd of the “apparent” H–H distances (eqs 1 and 2) with the experimental data as a function of the proportion p_B of a second population B ($\phi = 295^\circ$; $\psi = \psi_B$):

$$r_i^{\text{app}} = ((1 - p_B)r_{A_i}^{-6} + p_B r_{B_i}^{-6})^{-1/6} \quad (1)$$

$$\text{rmsd} = \sqrt{\sum_i [(r_i^{\text{app}} - r_i^{\text{exp}})^2]/n} \quad (2)$$

To obtain more clear results, only the six H–H distances depending on the angle ψ are taken into account in this calculation.²⁶ The contour plot representing this rmsd as a function of ψ_B and p_B is displayed in Figure 5. A unique minimum is observed, corresponding to a second population p_B of 60% having an angle ψ_B of 130° . The value of the minimal rmsd is 0.1 Å, which is a good result compared to the precedent value of 0.23 Å obtained after the simulated annealing procedure (corresponding to a mean Ψ angle of 24°). More interestingly, the total rmsd between experimental and simulated data for all distances that were used as constraints becomes now 0.09 Å instead of 0.18 Å (Figure 2B). This rmsd is almost equal to the partial rmsd for the “optimized” distances. Furthermore, the coupling constants back-calculated with the two-population hypothesis are now in good agreement with the experimental ones, as is attested by comparison of the first and last columns in Table 1. The two conformational families A and B are displayed in Figure 6. Concerning the ϕ and ψ angles, they are close to what was found for natural lactose,³¹ but their

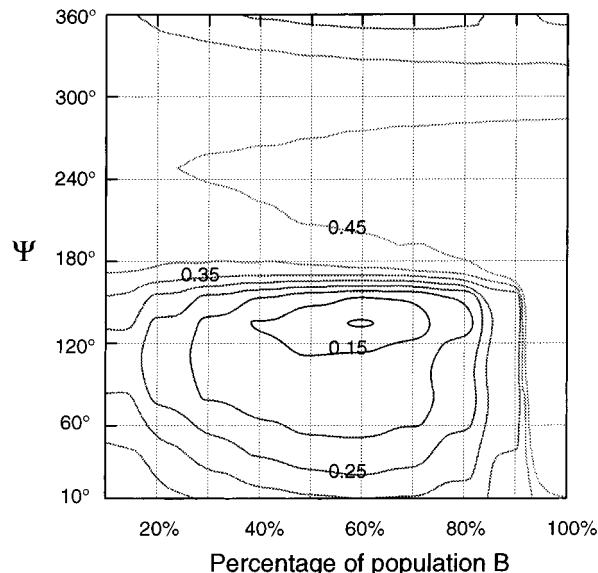


Figure 5. A 2D map of the rmsd (in angstroms) between the experimental H–H distances and the back-calculated ones with the two-population model as a function of p_B and ψ_B . p_B and ψ_B have been varied by steps of 10% and 5° , respectively.

relative proportion is different. However, contrary to previously published results,²⁷ the major conformation (population B) is the same for the natural and C-disaccharidic series. It is noticed that the nOe distances including the protons H6 of glucose have been back-calculated by variation of the dihedral angle χ and by averaging in r^{-6} of the resulting distances. A 80° value for χ under these conditions leads to the best agreement between experimental data and simulated ones. This result is coherent with the low value of J_{56} observed in the ^1H spectrum (1.7 Hz).

Conclusions

Although the experimental method used here is expected to give results more accurate than results from the classic approach, the general problem encountered during the study of solution structures of molecules by NMR is that the experimental data represent average values. As outlined by Ernst and co-workers,³² even if after molecular modeling the resulting structures fulfill all the experimental constraints, it does not prove that all conformational families are represented. To sample them more correctly, it is possible to use simulation procedures such as those employing time-³³ or ensemble-averaged³⁴ distance constraints or to work on distance subsets with cross-validation³⁵ or search algorithms.³² It can also be helpful to perform specific NMR experiments designed to detect particular internal motions. Off-resonance ROESY at various angles θ belongs in this category, since it provides information on the local dynamics of proton pairs.

Applied to the study of methyl β -C-lactoside in aqueous solution, this method has pointed out the presence of different internal motions. We have shown that this could be due to the

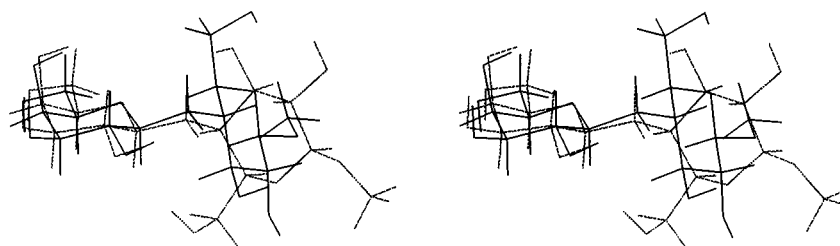


Figure 6. Stereoview of the two structural families A and B. In solid gray is structure A, and in black is structure B. The left is the galactose unit.

presence of two conformational families in fast exchange (nanosecond time scale). It appears that natural lactose and its synthetic analogue show common features not only for what concerns the anomeric and exoanomeric effects but also for the rather reduced mobility around ϕ . This can explain that the affinity for a lectine such as mucine³⁶ is identical for *C*-lactose and *O*-lactose. However, the proportion of conformational families having different Ψ is not identical between *C* and *O* series. Experiments are actually in progress in the laboratory to quantify these results via a comparative study.

Acknowledgment. The software used to process the off-resonance ROESY spectra has been kindly provided by Dr Hervé Desvaux.

Appendix

Obtaining Interproton Distances and Correlation Times from Off-Resonance ROESY Experiments. Details of the method transforming the measured cross-relaxation rates in interproton distances and correlation times have been described in refs 12–14. Let us summarize its principles. In our pulse scheme of off-resonance ROESY, dipolar relaxation along the effective field experienced by the protons is studied. The effective relaxation rates are thus weighted averages of the pure longitudinal and transverse relaxation rates as a function of the angle θ between this effective field and the static field axes. This angle is directly related to the rf offset Δ and rf field strength ω_1 by the relation $\tan \theta = \omega_1/\Delta$. Playing with one of these two parameters (or both) allows the accurate determination for each proton pair of both σ_{ij} and μ_{ij} —the pure longitudinal and transverse cross-relaxation rates, respectively. Without any assumption about the motion, they can be expressed as linear combinations of the spectral densities at particular frequencies:

$$\sigma_{ij} = -J_{ij}(0) + 6J_{ij}(2\omega) \quad (3)$$

$$\mu_{ij} = 2J_{ij}(0) + 3J_{ij}(\omega) \quad (4)$$

Assuming now that the motion of each proton pair can be adequately described by a monoexponential autocorrelation function, it is possible to write

$$J_{ij}(\omega) = \frac{\gamma^4 \hbar^2}{10r_{ij}^6} \frac{\tau_{c_{ij}}}{1 + \omega^2 \tau_{c_{ij}}^2} \quad (5)$$

From eqs 3–5, the interproton distance r_{ij} and the correlation time $\tau_{c_{ij}}$ can be extracted with high accuracy without the need of an internal reference.

Abbreviations and Acronyms

nOe	nuclear Overhauser effect
rmsd	root-mean-square deviation
COSY	correlation spectroscopy
ROESY	rotating-frame Overhauser effect spectroscopy

References and Notes

- (1) Rouzaud, D.; Sinaÿ, P. *J. Chem. Soc., Chem. Commun.* **1983**, 1353.
- (2) (a) Wu, T.-C.; Goekjian, P. G.; Kishi, Y. *J. Org. Chem.* **1987**, *52*, 4819. (b) Babirad, S. A.; Wang, Y.; Goekjian, P. G.; Kishi, Y. *J. Org. Chem.* **1987**, *52*, 4825. (c) Wang, Y.; Goekjian, P. G.; Ryckman, D. M.; Kishi, Y. *J. Org. Chem.* **1988**, *53*, 4151. (d) Miller, W. H.; Ryckman, D. M.; Goekjian, P. G.; Wang, Y.; Kishi, Y. *J. Org. Chem.* **1988**, *53*, 5582. (e) Wang, Y.; Babirad, S. A.; Kishi, Y. *J. Org. Chem.* **1992**, *57*, 468. (f) Haneda, T.; Goekjian, P. G.; Kim, S. H.; Kishi, Y. *J. Org. Chem.* **1992**, *57*, 490. (g) Goekjian, P. G.; Wu, T.-C.; Kang, H.-Y.; Kishi, Y. *J. Org. Chem.* **1987**, *52*, 4823.
- (3) Kishi, Y. *Pure Appl. Chem.* **1993**, *65*, 313.
- (4) Houk, K. N.; Eksterowicz, J. E.; Wu, Y.-D.; Fuglesang, C. D.; Mitchell, D. B. *J. Am. Chem. Soc.* **1993**, *115*, 4170.
- (5) Wei, A.; Boy, K. M.; Kishi, Y. *J. Am. Chem. Soc.* **1995**, *117*, 9432.
- (6) van Halbeek, H. *Curr. Opin. Struct. Biol.* **1994**, *4*, 697.
- (7) Tvaroska, I.; Hricovini, M.; Petrakova, E. *Carbohydr. Res.* **1989**, *189*, 359.
- (8) Dais, P. *Adv. Carbohydr. Chem. Biochem.* **1996**, *51*, 63.
- (9) All dihedral angles are defined according to the IUPAC Joint Commission on Biochemical Nomenclature (JCBN), *Symbols for Specifying the conformation of polysaccharide chains*, 1981 recommendation. Reproduced in *Eur. J. Biochem.* **1983**, *131*, 5. ϕ : (O5'-C1'-O4-C4); ψ : (C1'-O4-C4-C3); χ : (O5-C5-O6-C6).
- (10) (a) Bothner-By, A. A.; Stephens, R. L.; Lee, J.; Warren, C. D.; Jeanloz, R. W. *J. Am. Chem. Soc.* **1984**, *106*, 811. (b) Bax, A.; Davis, D. G. *J. Magn. Reson.* **1985**, *63*, 207.
- (11) Farmer, B. T., II; Macura, S.; Brown, L. R. *J. Magn. Reson.* **1987**, *72*, 347.
- (12) Desvaux, H.; Berthault, P.; Birlirakis, N.; Goldman, M. *J. Magn. Reson., Ser. A* **1994**, *108*, 219.
- (13) Desvaux, H.; Berthault, P.; Birlirakis, N. *Chem. Phys. Lett.* **1995**, *233*, 545.
- (14) Berthault, P.; Birlirakis, N.; Rubinstenn, G.; Sinaÿ, P.; Desvaux, H. *J. Biomol. NMR* **1996**, *8*, 23.
- (15) Rubinstenn, G. PhD Thesis, University of Paris VI, 1996.
- (16) Shaka, A. J.; Freeman, R. *J. Magn. Reson.* **1983**, *51*, 169.
- (17) Wagner, G. *J. Magn. Reson.* **1983**, *55*, 151.
- (18) Desvaux, H.; Berthault, P.; Birlirakis, N.; Goldman, M.; Piotto, M. *J. Magn. Reson., Ser. A* **1995**, *113*, 47.
- (19) Desvaux, H.; Goldman, M. *J. Magn. Reson., Ser. B* **1996**, *110*, 198.
- (20) Emsley, L.; Bodenhausen, G. *J. Magn. Reson.* **1989**, *82*, 211.
- (21) Press, W. H.; Flannery, B. P.; Teukolsky, S. A.; Vetterling, W. T. *Numerical Recipes in C. The art of scientific programming*; Cambridge University Press: Cambridge, U.K., 1988.
- (22) Brünger, A. T. *X-plor Version 3.1, a System for X-Ray Crystallography and NMR*; Yale University Press: New Haven and London, 1992.
- (23) Biosym/MSI, 9685 Scranton Road, San Diego, CA 92121-3752.
- (24) Maple, J. R.; Hwang, M. J.; Stockfisch, T. P.; Dinur, U.; Woldman, M.; Ewig, C. S.; Hagler, A. T. *J. Comput. Chem.* **1994**, *15*, 162.
- (25) Haasnoot, C. A. G.; de Leeuw, F. A. A. M.; Altona, C. *Tetrahedron* **1980**, *36*, 2783.
- (26) Two interactions involving the protons H6 of glucose (H6-H_{link}' and H6',H5-H_{link}) have been discarded for the rmsd calculation, although the values of ψ influence them. The reason is that a small variation of the angle χ , for which too imprecise data are available, leads to dramatic variation of these distances.
- (27) Espinosa, J.-F.; Martín-Pastor, M.; Asensio, J. L.; Dietrich, H.; Martín-Lomas, M.; Schmidt, R. R.; Jiménez-Barbero, J. *Tetrahedron. Lett.* **1995**, *36*, 6329.
- (28) Only the β isomer was taken into account.
- (29) Allinger, N.; Yuh, Y. H.; Lii, J.-H. *J. Am. Chem. Soc.* **1989**, *111*, 8551.
- (30) *The nuclear Overhauser effect in structural and conformational analysis*; Neuhaus, D., Williamson, M. P., Eds.; VCH Publishers: New York, 1989.
- (31) (a) Fernández, P.; Jiménez-Barbero, J. *Carbohydr. Res.* **1993**, *248*, 15. (b) Asensio, J. L.; Jiménez-Barbero, J. *Biopolymers* **1995**, *35*, 55. (c) Engelsens, S. B.; Koca, J.; Braccini, I.; Hervé du Penhoat, K.; Pérez, S. *Carbohydr. Res.* **1995**, *276*, 1.
- (32) Brüschweiler, R.; Blackledge, M.; Ernst, R. R. *J. Biomol. NMR* **1991**, *1*, 3.
- (33) Torda, A. E.; Scheek, R. M.; van Gunsteren, W. F. *J. Mol. Biol.* **1990**, *214*, 223.
- (34) Wang, J.; Hodges, R. S.; Sykes, B. D. *J. Am. Chem. Soc.* **1995**, *117*, 8627.
- (35) Bonvin, A. M. J. J.; Brünger, A. T. *J. Biomol. NMR* **1996**, *7*, 72.
- (36) Espinosa, J.-F.; Cañada, F. J.; Asensio, J. L.; Dietrich, H.; Martín-Lomas, M.; Schmidt, R. R.; Jiménez-Barbero, J. *Angew. Chem., Int. Ed. Engl.* **1996**, *39*, 303.